Title

Case Report: Multimodal, Longitudinal Assessment of Retinal Structure and Function following Laser Retinal Injury.

Journal

Optometry and Vision Science, 100(4)

Authors

Wang, Yiyi

La, Tammy

Tuten, William

et al.

Publication Date

2023-04-01

DOI

10.1097/OPX.0000000000002004

Peer reviewed

HHS Public Access

Author manuscript

Optom Vis Sci. Author manuscript; available in PMC 2024 April 01.

Published in final edited form as:

Optom Vis Sci. 2023 April 01; 100(4): 281–288. doi:10.1097/OPX.0000000000002004.

Case Report: Multimodal, Longitudinal Assessment of Retinal Structure and Function following Laser Retinal Injury

Yiyi Wang, OD, FAAO,

Tammy T. La, OD,

Melanie Mason, OD, FAAO,

William S. Tuten, OD, PhD,

Austin Roorda, PhD

Herbert Wertheim School of Optometry & Vision Science, University of California, Berkeley, Berkeley, California

Abstract

Significance.—This case report demonstrates the use of novel imaging techniques and functional tests to longitudinally evaluate retinal structure and function after laser retinal injury. The structural and functional prognosis could be predicted with clinical findings, high-resolution retinal imaging, and functional testing.

Purpose.—We present a laser retinal injury case in which an adaptive optics scanning laser ophthalmoscope and adaptive optics-based psychophysics were used to examine and monitor retinal structure and function after accidental exposure to a 1-W infrared laser beam.

Case Report.—A 23-year-old patient was unwittingly exposed to a 1-W, 852-nm continuous-wave laser at work as they noticed a small central blurry spot in the right eye. An initial eye examination was done 1 day after exposure, and the right eye's acuity was $20/25^{-2}$. Posterior segment evaluation revealed disrupted outer retina near the right eye's fovea. Adaptive optics imaging 2 weeks after the exposure revealed a $0.50 \times 0.75°$ elliptical area with irregular borders and abnormal cone reflectivity just below the fovea. Starting at one-month follow-up, structural recovery was observed on optical coherence tomography (OCT). Subsequent adaptive optics imaging showed significant recovery of cone reflectivity. Importantly, adaptive optics microperimetry showed measurable detection thresholds at all affected retinal locations at 6 months. By 10 months, all sites exhibited normal sensitivities.

Conclusions.—Retinal structure and function from laser injury can be visualized and measured with OCT, adaptive optics imaging and psychophysics. An intact Bruch's membrane on OCT and measurable retinal sensitivity by adaptive optics microperimetry may serve as good biomarkers for retinal recovery.

Lasers are widely used in academic, laboratory, medical, and industrial settings. Owing to the ability to collimate and focus lasers to extremely high irradiances, they can cause injury, including damage to retinal tissue. Even relatively low-power laser pointers can cause retinal

Corresponding author: Yiyi Wang, yiyiwang@berkeley.edu.

injury if misused. The extent of ocular damage depends on the duration of exposure and the properties of the laser, such as beam diameter, beam vergence, wavelength, and power output.[1–3]

Laser light damage can occur by three mechanisms: photothermal, photomechanical, or photochemical.[2–3] Photothermal damage occurs when the energy from the laser is transferred to the pigment of the cells as heat, causing protein denaturation and cell death. Photochemical damage occurs when laser energy causes photochemical reactions, such as breakage of bonds or creation of reactive oxidative species. Photomechanical damage occurs when high-irradiance laser exposures over a short pulse duration induce plasma and water vaporization, leading to tissue disruption.[2] Laser damage is wavelength dependent: laser damage thresholds for shorter wavelengths are more likely to be photochemical than photothermal, whereas the photothermal injury is generally the case for longer wavelengths, including near-infrared wavelengths.[4–5] Laser damage is also tissue dependent: foveal pigment and melanin in the retinal pigment epithelium, for example, absorb more light than other tissues and are therefore more prone to damage.[2] Finally, cells like photoreceptors can suffer collateral damage when cells that they rely on, such as retinal pigment epithelium, are the primary site of damage.[2]

Laser-induced injury can be clinically evaluated and diagnosed with dilated fundus examination, fundus imagery, and spectral-domain optical coherence tomography (SD-OCT), but the resolution of clinical imaging is limited. Furthermore, clinical functional tests including visual acuity and visual field do not provide information about the damaged retina at the cellular level.

Here, we present a longitudinal data on a laser eye injury case from laboratory laser exposure to a 1-W 852-nm continuous-wave laser beam. Our data include results from three conventional clinical eye examinations in addition to results from four research laboratory visits for high-resolution assessments of structure and function.

High-resolution retinal imaging of the outer retinal structure in and around the lesion area was done with an adaptive optics scanning laser ophthalmoscope with a confocal detector configuration. Adaptive optics scanning laser ophthalmoscopy can resolve the cone photoreceptor mosaic by measuring and optically correcting for blur-causing aberrations in the human eye. An 840-nm light was used to record a series of 0.9 × 0.9° videos of the retina with a 30-Hz frame rate at a series of retinal locations at and around the lesion. Images generated from each video were stitched together to form a high-resolution montage.

Assessment of the preferred retinal locus was done by recording a video with 840-nm light while the patient fixated on a small, blinking 680-nm spot delivered via the same laser raster scan. The exact retinal locations where the stimulus landed during fixation over the course of a video were used to determine the mean preferred retinal locus and the fixation stability. Fixation stability was indicated by computing an isodensity contour line that contained 68% of the blinking spot locations.

Adaptive optics-corrected visual acuity measurements were made on the same platform wherein an adaptive-optics-corrected decrement letter was delivered on an infrared

background, accomplished by modulating the 840-nm raster at appropriate time points within the scan.[6] Acuity was determined using a 4-alternative forced choice, tumbling-E paradigm and used a 30-trial adaptive staircase guided by the Quest algorithm.[7]

Adaptive optics microperimetry with real-time eye tracking was used to examine the retinal sensitivity of the damaged area with small, retinally stabilized increment stimuli.[8] The retinal imaging and tracking were done with 840-nm light, and a 3-arcmin, green (543 nm) stimulus was presented at targeted locations via the same raster scan. The vergence of the green channel was set to offset the eye's native longitudinal chromatic aberration, ensuring that the microperimetry stimulus was focused on the same plane as the infrared imaging light. The test locations were manually selected by the experimenters. Retinal sensitivity at each location was measured using a yes-no Quest adaptive staircase procedure (40 trials per location). A larger 1.7 × 1.7° imaging field of view was used to ensure more robust tracking from trial to trial.

One-second retinal videos were recorded during each adaptive optics-based visual acuity and microperimetry trial to recover the exact stimulus position on the retina and to gauge tracking fidelity.

CASE REPORT

Initial Clinical Visit (1 Day after Exposure)

A 23-year-old patient presented to the University Eye Clinic with a chief complaint of a small central blurry spot of the right eye from workplace laser exposure less than 24 hours prior. The patient was an optics researcher doing visual inspection on the optical table, unaware that a 1-W Titanium-Sapphire (852 nm) continuous-wave laser was on and directed into their right eye. The estimated exposure time was up to 10 seconds. The patient did not recall any visible acute exposure but did report some visual disturbances while doing the inspection and immediately thereafter. The patient reported an unremarkable past ocular and systemic history.

The complete timeline of clinical visits and research lab visits is shown in Figure 1. The patient's unaided visual acuity was 20/30 in the right eye and $20/20^{-2}$ in the left eye. With pinhole, the acuity improved to $20/25^{-2}$ and $20/20^{-}$ respectively. Anterior segment findings included mild blepharitis and mild papillary reaction on palpebral conjunctiva of both eyes. Intraocular pressure was 18 mmHg in each eye with Goldmann tonometry. On an Amsler grid, the patient reported that their right eye had a small area of distortion slightly superior to fixation with a size of one grid square, about 1° equivalently. The patient elected to have only the right eye dilated with 1% tropicamide and 2.5% phenylephrine. The dilated fundus examination of the right eye revealed a small yellow lesion slightly inferior to the fovea, with no associated intraretinal fluid or hemorrhage (Figure 2A). Fundus autofluorescence showed an oval-shaped hypofluorescence in the right eye, co-localized with the yellow lesion on the fundus photo. Spectral-domain optical coherence tomography (SD-OCT) macular scans showed slight elevation and disruptions of the foveal outer retinal bands corresponding to the external limiting membrane, the photoreceptor inner segment/outer segment junction, and the cone outer segment tips. More notably, atypical

hyperreflective structures were observed at the fovea, extending inward from the retinal pigment epithelium through all outer retinal layers and terminating at the outer plexiform layer. The hyperreflective band traced a path that was similar to the central photoreceptor axons comprising the Henle fiber layer (Figure 3A). Bruch's membrane remained intact as there was no strong choroidal signal seen beneath the fovea. The patient's left eye was unremarkable with undilated ophthalmoscopic examination.

The patient was diagnosed with laser-induced maculopathy of the right eye, and no treatment was indicated. The patient was educated on the importance of using protective eyewear during laser-related research work, advised to monitor visual symptoms with an at-home Amsler grid, and instructed to return immediately if they noticed any vision change; otherwise, the patient was scheduled to return in 1 month for a follow-up visit.

First Research Lab Visit (17 Days after Exposure)

The patient consented to undergo a research protocol for evaluating retinal structure and function longitudinally at the cellular level. Adaptive optics scanning laser ophthalmoscope confocal imaging, preferred retinal locus assessment, and adaptive optics-corrected visual acuity were performed at the initial research lab visit.

Adaptive optics scanning laser ophthalmoscope confocal imaging revealed a 0.50 × 0.75° elliptical retinal area with irregular borders slightly inferior to the fixation (Figure 4A), which corresponded to the disrupted area found on SD-OCT (Figure 3A), and fundus autofluorescence (Figure 2A). The lesion showed abnormal cone reflectivity with hyperreflective and hyporeflective patches lacking a typical, unambiguous, contiguous cone mosaic pattern. The average location of the preferred retinal locus (yellow dot) was at the upper edge of the lesion and the distribution of the preferred retinal locus (yellow contour) was relatively high, encompassing about 0.5° (Figure 4A). Adaptive optics-corrected visual acuity result was 20/18.

2nd Clinical Visit (28 Days after Exposure)

The patient reported that the distortion in their right eye had improved slightly. The pinhole visual acuity was $20/25^{+2}$ in the right eye and 20/20 in the left eye. The patient declined pupil dilation at this visit. Small pupil evaluation revealed a mild improvement of the right eye's yellow lesion. Fundus photos and fundus autofluorescence also confirmed the reduction in size of the lesion (Figure 2B). The SD-OCT macular scan showed resolution of the hyperreflective structures that were seen in the outer retinal layers at the first clinical visit. Central, small areas of external limiting membrane and photoreceptor inner segment/outer segment junction line disruption by a small hyperreflective clump indicated possible retinal pigment epithelium migration. Two narrow streaks of higher choroidal signal beneath the edges of the clump indicated possible minor breaks in the Bruch's membrane and/or retinal pigment epithelium (Figure 3B).

The patient was advised that the retinal injury could either continue to resolve over time or remain stable but was unlikely to worsen. No treatment was indicated at this time and the patient was instructed to continue monitoring their visual symptoms at home with Amsler grid and to return in 3–4 months for a follow-up visit.

2nd Research Lab Visit (119 Days after Exposure)

Adaptive optics scanning laser ophthalmoscope confocal imaging, preferred retinal locus assessment, and adaptive optics-corrected visual acuity were performed at the second research visit. Compared with the initial visit, the adaptive optics confocal images collected at follow-up showed that the cone reflectivity was restored in some regions that previously appeared disrupted. (Figure 4B). The preferred retinal locus at the second research visit showed a more regular and tighter fixation pattern compared to the initial visit. The adaptive-optics-corrected visual acuity was relatively unchanged (20/18 at the 1st visit and 20/21 at the 2nd visit) whereas the eye motions were similar between the two visits during the acuity task.

Adaptive optics microperimetry was attempted at this visit, but results were discarded for two reasons. First, the field size for retinal imaging and tracking was 0.9 × 0.9° which led to multiple tracking failures. Second, the 543-nm power level was set too high, and so all thresholds were very close to the lowest control values of the laser modulator. These low control levels are most susceptible to non-linearities in the laser control calibration. Both problems were corrected for research lab visits 3 and 4.

3rd Clinical Visit (189 Days after Exposure)

The patient reported subjective improvement in right eye's vision since the last clinical visit, noticing only a slight distortion when viewing monocularly with the right eye. The patient's best-corrected visual acuity of the right eye improved to 20/20^{-}. Fundus photography and fundus autofluorescence showed a smaller lesion than previous visits (Figure 2C). The SD-OCT macular scan showed a smaller hyperreflective clump at the fovea than the previous visit. Small areas of photoreceptor inner segment/outer segment junction disruption remained present at the fovea. The choroid signals appeared less strong than the second clinical visit (Figure 3C). The patient's ocular health was otherwise normal. The patient was advised to continue to monitor symptoms at home and return as needed.

3rd Research Lab Visit (191 Days after Exposure)

Adaptive optics scanning laser ophthalmoscope confocal imaging, preferred retinal locus assessment, adaptive optics-corrected visual acuity and adaptive optics microperimetry were performed at the 3rd research visit. Adaptive optics images showed continuing recovery of the cone reflectivity from the 2nd visit (Figure 4C). Preferred retinal locus measurements showed similarly tight and stable fixational patterns as the 2nd visit. Adaptive-optics-corrected visual acuity was 20/16, stable if not improved from previous visits. Adaptive optics microperimetry measurements were made at three visible lesion sites, the fovea, and at two sites with normal-appearing cones at similar retinal eccentricities. Importantly, all affected retinal locations showed measurable retinal sensitivity (Figure 5A). The largest remaining lesion (L1) corresponding to outer retina disruption at the fovea on OCT (Figure 3C) had significantly reduced sensitivity. All other affected areas had slightly reduced retinal sensitivity compared with nearby undamaged areas, suggesting that they were on a path to near or full recovery.

4th Research Lab Visit (265 Days after Exposure)

For the fourth and final research visit, the same experimental procedures were performed as in research lab visit 3. Adaptive optics images showed slightly improved cone reflectivity since the 3rd visit (Figure 4D). The preferred retinal locus pattern was stable from before. Adaptive optics-corrected visual acuity was also stable, measured as 20/18. Adaptive optics microperimetry was performed at similar locations (fovea, 2 areas with normal cone reflectivity, and 3 areas with visible lesions). All areas with visible hypo- or hyper-reflective lesions showed similar retinal sensitivity as the nearby unaffected area, indicating functional recovery (Figure 5B).

DISCUSSION

A recovery of retinal structure and function of this laser retinal injury case was observed longitudinally. Adaptive optics scanning laser ophthalmoscope confocal images showed structural recovery in cone reflectivity, and OCT scans showed improvement of the outer retinal structures. Adaptive optics-corrected visual acuity showed stable acuity measurement throughout the 10-month period. The preferred retinal locus showed an improved fixational pattern at 1 month and adaptive optics microperimetry demonstrated functional recovery at 10 months. Given that the injury in our case was from a continuous-wave, near-infrared source and given the nature of the lesion appearance and its recovery, the mechanism for damage in our patient was almost certainly photothermal.

What Are the Hyperreflective Structures Observed on OCT?

In our patient's OCT image, the hyperreflective structures extended radially from the foveal center following a trajectory like the photoreceptor axons that form the Henle fiber layer. The presence of such characteristic findings could indicate the inflammation and swelling of the photoreceptors and retinal pigment epithelium. The hyperreflective structures observed on OCT were previously reported to arise from damage and consequent increased scattering of the Henle fiber layer,[9–10] possibly because of direct injury from the laser exposure or as a result of transneuronal degeneration.[3] An alternative hypothesis was that retinal stress induces a change in the cytoplasmic refractive index of the Müller cells, which extend through the entire retina and travel in parallel with cone axons.[3] In our patient and previous case reports,[9–10] it has been found that the hyperreflectivity can resolve after 1 month. Tomasso et al. also reported the hyperreflective structures could affect deeper layers as they found rarefactions in the choriocapillaris corresponding to the damaged sites using OCT angiography, but optical artifacts cannot be ruled out due to the overlaying hyperreflectivities.[10]

Management of Laser Retinal Injury

Currently, there is no standard of care or treatment of laser retinal injury.[5] In general, most of the reported laser retinal injury cases showed reversible retinal damage with corticosteroid or surgical treatment, although having a permanent scotoma was also not uncommon.[5, 11–15] Previous literature showed the managements of laser retinal damage cases including observation,[9] oral corticosteroid,[1,12–15] and surgical intervention,[11] depending on the injury severity.

In severe cases of laser injury where preretinal hemorrhage and macular hole occur, surgical intervention is necessary. Nd:YAG hyaloidotomy can be used to treat preretinal/subhyloid hemorrhage, and vitrectomy can be used to close a full-thickness macular hole.[11]

In milder cases where surgeries are not indicated, evidence-based medical intervention is limited. Several studies showed visual and structural improvement with a short course of oral corticosteroid treatment immediately after the laser exposure.[1, 12–15] The corticosteroid was suggested to reduce inflammatory response by decreasing the retinal pigment epithelium migration and proliferation in response to the laser-related injury.[12–13] Further study comparing steroid use and observation only would shed light on whether steroid treatment would be indicated. In addition, lutein was used in a case of laser damage as it has antioxidant and anti-inflammatory effects in other macular diseases, and the visual outcome was comparable to steroid treatment.[16] Because of the lack of a control group, it is difficult to confirm if the structural and visual improvement observed in patients was truly attributed to the corticosteroids or lutein intake, or the natural course of the retinal recovery.

One longitudinal study found continual structural and visual recovery over a 4-year period.[15] The factors that may promote recovery include an intact Bruch's membrane, laser exposure at a young age, exposure to a long wavelength as opposed to a short wavelength, and early corticosteroid treatment.[15] An intact Bruch's membrane was suggested to support healing of the damaged retinal pigment epithelium cells, in turn promoting recovery of the damaged retinal tissue.[15,17]

Our patient had all the factors that were suggested to promote recovery, aside from the corticosteroid treatment. The exposure was to an infrared, continuous-wave laser; Bruch's membrane was left largely intact; there was no preretinal hemorrhage or maccular hole; and visual acuity was only mildly reduced at the onset. As anticipated, they showed continued recovery of a normal-appearing retina on SD-OCT and adaptive optics confocal images. The hyperreflective structures resolved after 28 days on SD-OCT with evidence of small areas of retinal pigment epithelium cell migration into the outer retinal space, which resolved at the 6-month (189 days) follow-up (Figure 3A–C). The adaptive optics confocal images at 6 months (191 days) showed a slightly smaller lesion size (L1) comparing to the 4-month (119 days) visit Figure 4C. Another case report visualizing laser retinal injury with adaptive optics imaging showed a decrease in lesion size from 11 months to 20 months post exposure.[18] From 6-month (191 days) to 10-month (265 days) research lab visits, our patient showed improvement of retinal sensitivity measured with adaptive optics microperimetry, whereas retinal appearance remained relatively stable.

Limitations

We did not correct for transverse chromatic aberration of the patient's eye while performing adaptive optics microperimetry because of limited experiment time, and because we did not want the required bright green imaging light to cause any unnecessary discomfort to the patient.[19] We do not see this as major limitation, however, because the average transverse chromatic aberration in a human in the foveal region is about 2 arcmin,[20] which is smaller than the size of the stimulus itself and is too small to cause the stimulus to fall outside of any of the visible lesions.

CONCLUSIONS

Retinal structure and function from laser injury can be visualized and measured with OCT, adaptive optics imaging and psychophysics. Medical and surgical treatments are indicated in severe cases when intraocular hemorrhage is observed. Our study shows that, in milder cases, observation is sufficient and natural recovery of the injury site can be confirmed with an intact Bruch's membrane on OCT and measurable retinal sensitivity by adaptive optics microperimetry.

ACKNOWLEDGMENTS

Written informed consent was obtained for identifiable health information included in this case report. No identifiable health information was included in this case report.

This research was supported by the NEI Bioengineering Partnership Grant R01EY023591, the American Academy of Optometry Foundation Ezell Fellowship, the Hellman Fellows Fund, and the Alcon Research Institute Young Investigator Award.

REFERENCES

1. Marinescu AI, Hall CM. Laser-Induced Maculopathy and Outcomes After Treatment with Corticosteroids and Lutein. Cureus 2021;13:e18470. [PubMed: 34692258]
2. Barkana Y, Belkin M. Laser Eye Injuries. Surv Ophthalmol 2000;44:459–78. [PubMed: 10906379]
3. Pocock GM, Oliver JW, Specht CS, et al. High-Resolution in Vivo Imaging of Regimes of Laser Damage to the Primate Retina. J Ophthalmol 2014;2014:516854. [PubMed: 24891943]
4. Ham WT Jr, Ruffolo JJ Jr, Mueller HA, et al. Histologic Analysis of Photochemical Lesions Produced in Rhesus Retina by Short-wavelength Light. Invest Ophthalmol Vis Sci 1978;17:1029–35. [PubMed: 100464]
5. Neffendorf JE, Hildebrand GD, Downes SM. Handheld Laser Devices and Laser-induced Retinopathy (LIR) in Children: An Overview of the Literature. Eye 2019;33:1203–14. [PubMed: 30894692]
6. Foote KG, Loumou P, Griffin S, et al. Relationship between Foveal Cone Structure and Visual Acuity Measured with Adaptive Optics Scanning Laser Ophthalmoscopy in Retinal Degeneration. Invest Ophthalmol Vis Sci 2018;59:3385. [PubMed: 30025078]
7. Watson AB, Pelli DG. QUEST: a Bayesian Adaptive Psychometric Method. Percept Psychophys 1983;33:113–20. [PubMed: 6844102]
8. Tuten WS, Tiruveedhula P, Roorda A. Adaptive Optics Scanning Laser Ophthalmoscope-Based Microperimetry. Optom Vis Sci 2012;89:563–74. [PubMed: 22446720]
9. Bhavsar KV, Wilson D, Margolis R, et al. Multimodal Imaging in Handheld Laser-induced Maculopathy. Am J Ophthalmol 2015;159:227–31.e2. [PubMed: 25448992]
10. Tomasso L, Benatti L, La Spina C, et al. Optical Coherence Tomography Angiography Findings in Laser Maculopathy. Eur J Ophthalmol 2017;27:e13–e5. [PubMed: 28009410]
11. Alsulaiman SM, Alrushood AA, Almasaud J, et al. High-Power Handheld Blue Laser-induced Maculopathy: The Results of the King Khaled Eye Specialist Hospital Collaborative Retina Study Group. Ophthalmology 2014;121:566–72.e1. [PubMed: 24184164]
12. Lee GD, Baumal CR, Lally D, et al. Retinal Injury after Inadvertent Handheld Laser Exposure. Retina 2014;34:2388–96. [PubMed: 25380069]
13. Chen YY, Lu N, Li JP, et al. Early Treatment for Laser-induced Maculopathy. Chin Med J (Engl). 2017;130:2121–2. [PubMed: 28836559]
14. Mtanes K, Mimouni M, Zayit-Soudry S. Laser Pointer-induced Maculopathy: More Than Meets the Eye. J Pediatr Ophthalmol Strabismus 2018;55:312–8. [PubMed: 29913024]
15. Chen X, Dajani O, Alibhai AY, et al. Long-term Visual Recovery in Bilateral Handheld Laser Pointer-induced Maculopathy. Retin Cases Brief Rep 2021;15:536–9. [PubMed: 30640318]

16. Zhao N, Liu L. Long-Term Changes in Optic Coherence Tomography in a Child with Laser Pointer Maculopathy: A Case Report and Mini Review. Photodiagnosis Photodyn Ther 2017;18:264–6. [PubMed: 28347866]

17. Dhakal KR, Walters S, McGregor JE, et al. Localized Photoreceptor Ablation Using Femtosecond Pulses Focused with Adaptive Optics. Transl Vis Sci Technol 2020;9:16.

18. Vitellas C, Doble N, Wells-Gray EM, et al. Cone Photoreceptor Integrity Assessed with Adaptive Optics Imaging after Laser Pointer-induced Retinal Injury. Retin Cases Brief Rep 2022;16:586–92 [PubMed: 32541434]

19. Harmening WM, Tiruveedhula P, Roorda A, Sincich LC. Measurement and Correction of Transverse Chromatic Offsets for Multi-wavelength Retinal Microscopy in the Living Eye. Biomed Opt Express 2012;3:2066–77. [PubMed: 23024901]

20. Winter S, Sabesan R, Tiruveedhula P, et al. Transverse Chromatic Aberration Across the Visual Field of the Human Eye. J Vis 2016;16:9.

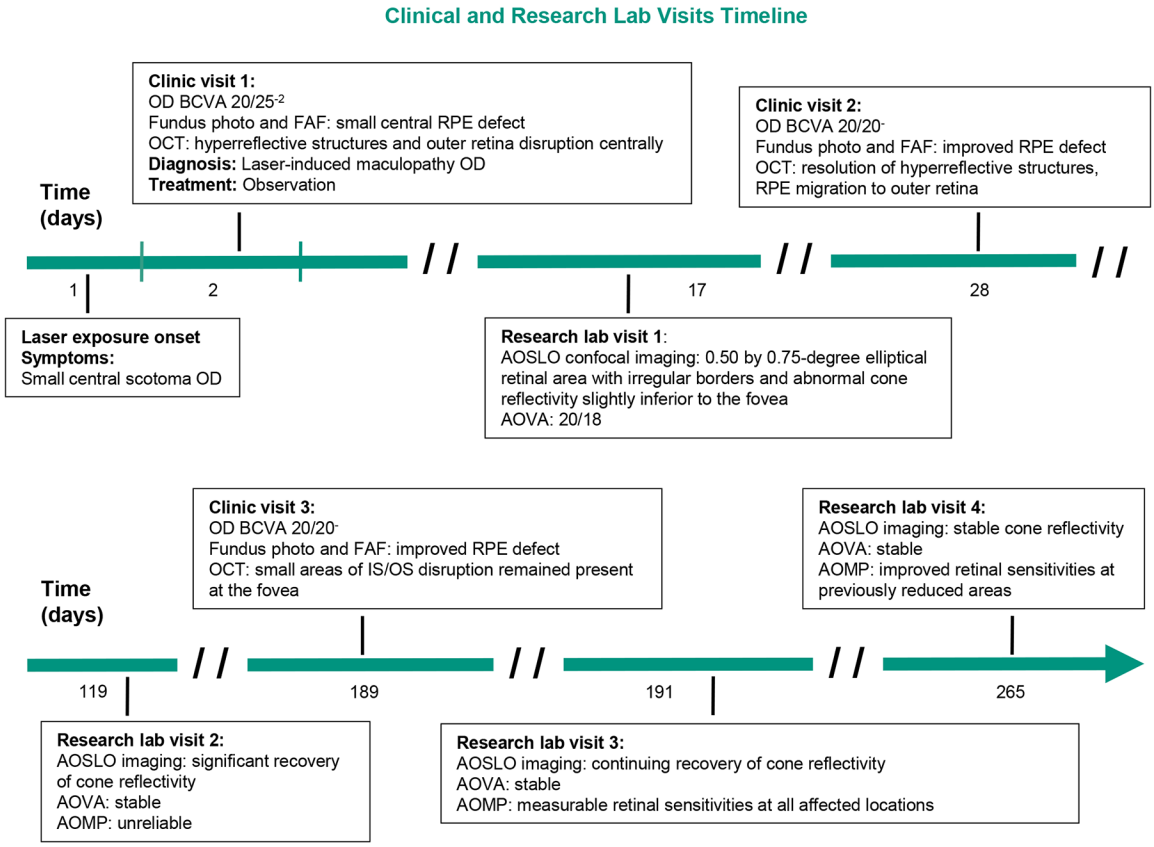

Figure 1.

Clinical timeline: a 23-year-old patient was diagnosed and monitored for laser retinal injury. AOMP = adaptive optics microperimetry; AOSLO = adaptive optics scanning laser ophthalmoscope; AOVA = adaptive optics–corrected visual acuity; BCVA = best-corrected visual acuity; FAF = fundus autofluorescence; IS/OS = inner segment/outer segment; OCT = optical coherence tomography; OD = right eye; RPE = retinal pigment epithelium.

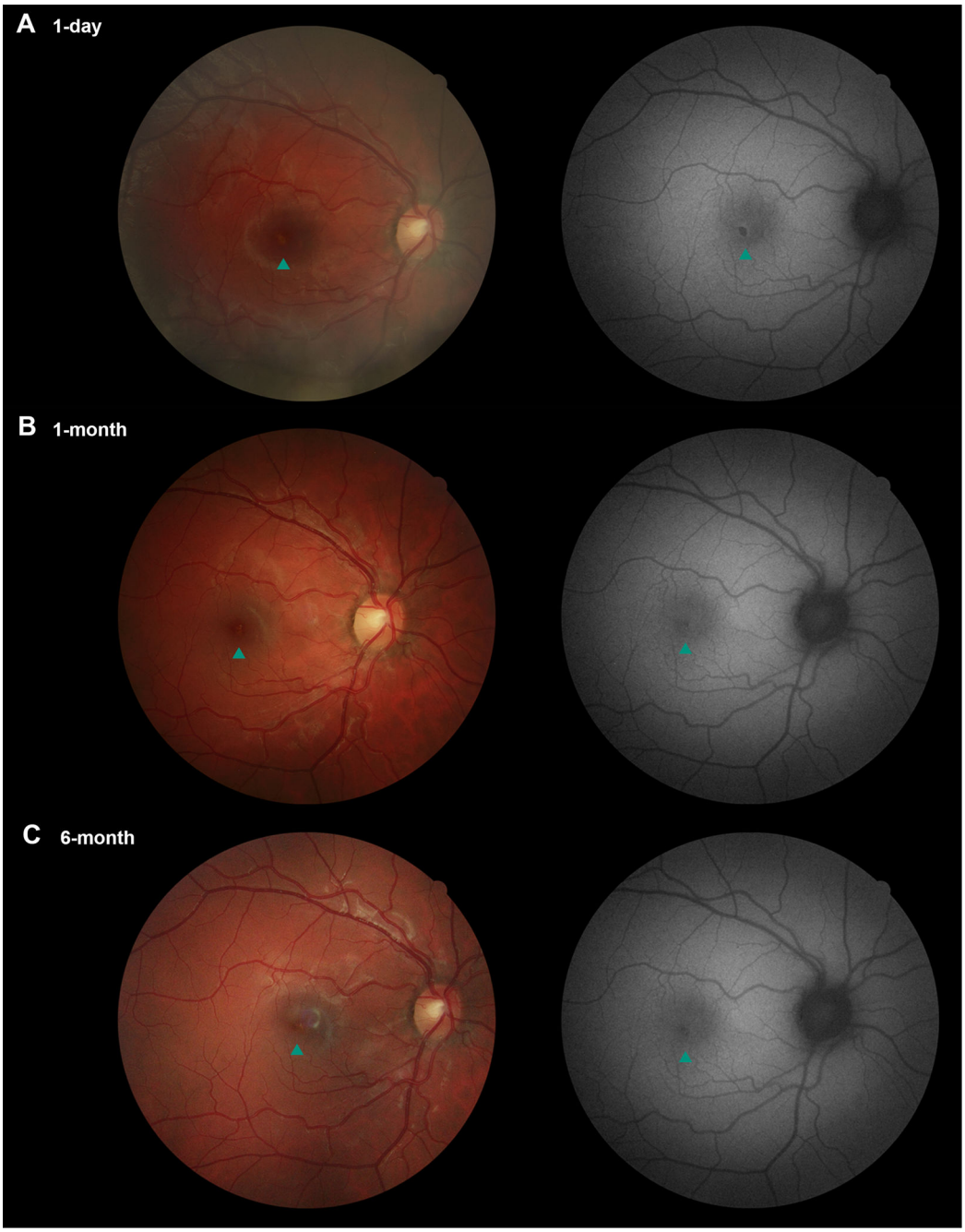

Figure 2.

Color fundus photos and fundus autofluorescence from all 3 clinical visits. The green arrowheads pointed up towards the lesion. Timelines were indicated on each image. The color fundus photos showed a yellow lesion inferior to fovea in panel A and the lesion size was reduced across subsequent visits. The hyporeflective area on fundus autofluorescence corresponded with the yellow lesion observed on color fundus photos, which also improved over time.

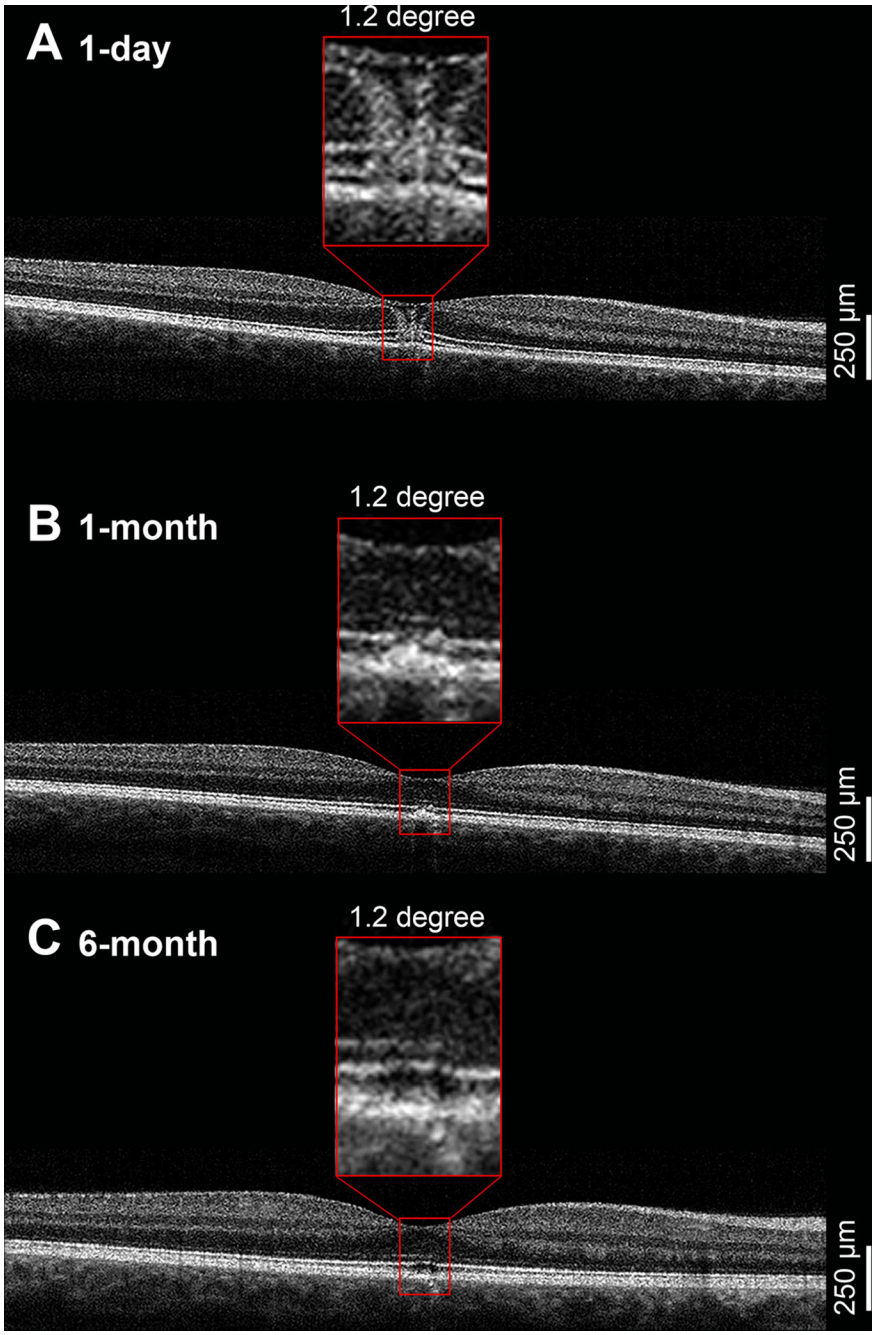

Figure 3.

Spectral-domain optical coherence tomography (SD-OCT) from all 3 clinical visits. Timelines were indicated on each image. Enlarged views of the lesions found on OCT were shown in each inset. Red boxes represent a 1.2° width on the OCT. Vertical scale bar length represented 250 µm.

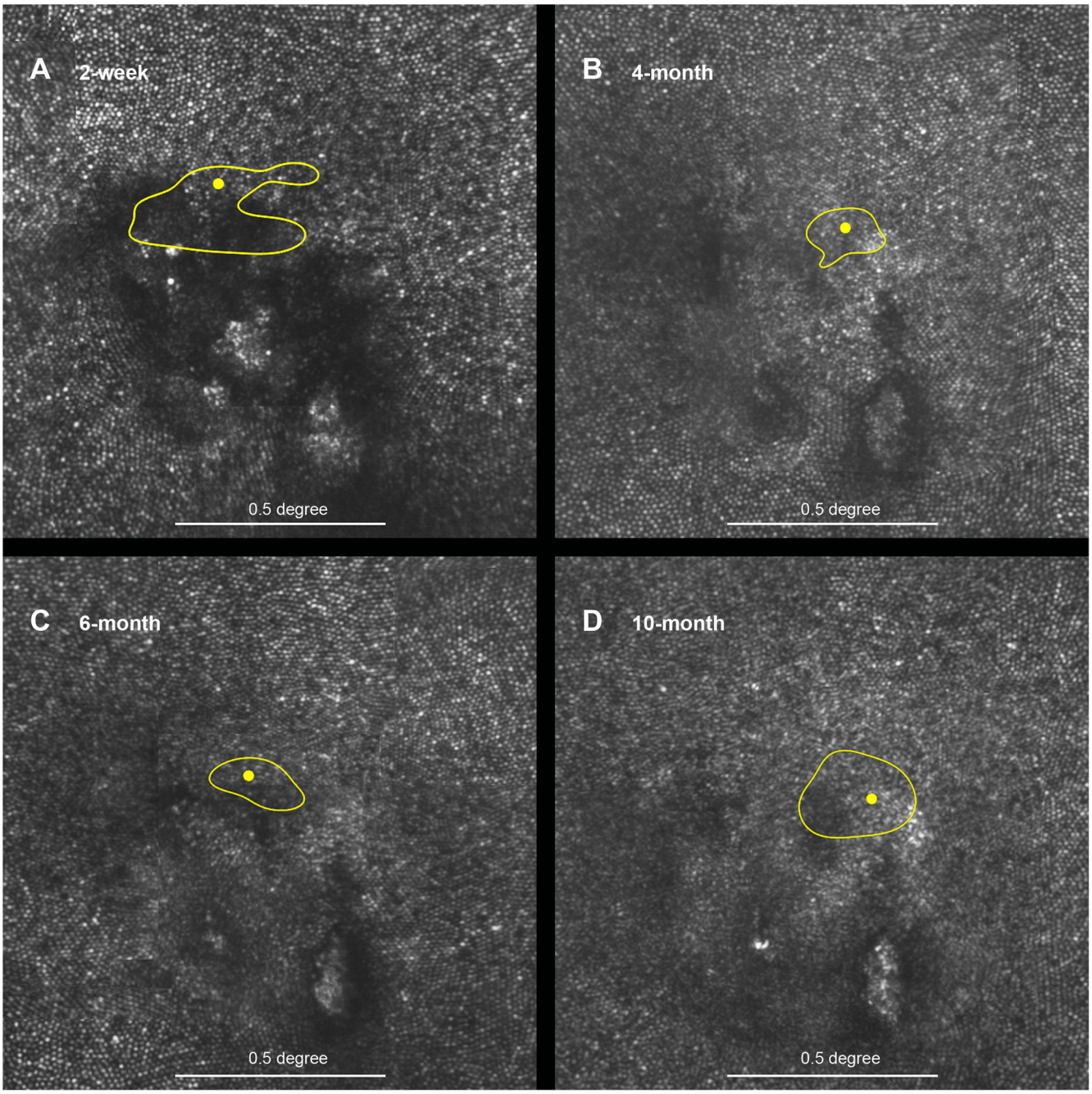

Figure 4.

Adaptive optics scanning laser ophthalmoscope confocal images of the lesion area from 4 research visits. Timeline and scale bar were labeled on the images. Yellow contours showed the non-uniform isoline contours that encompassed 68% of the eye traces with average preferred retinal locus labeled with a yellow dot.

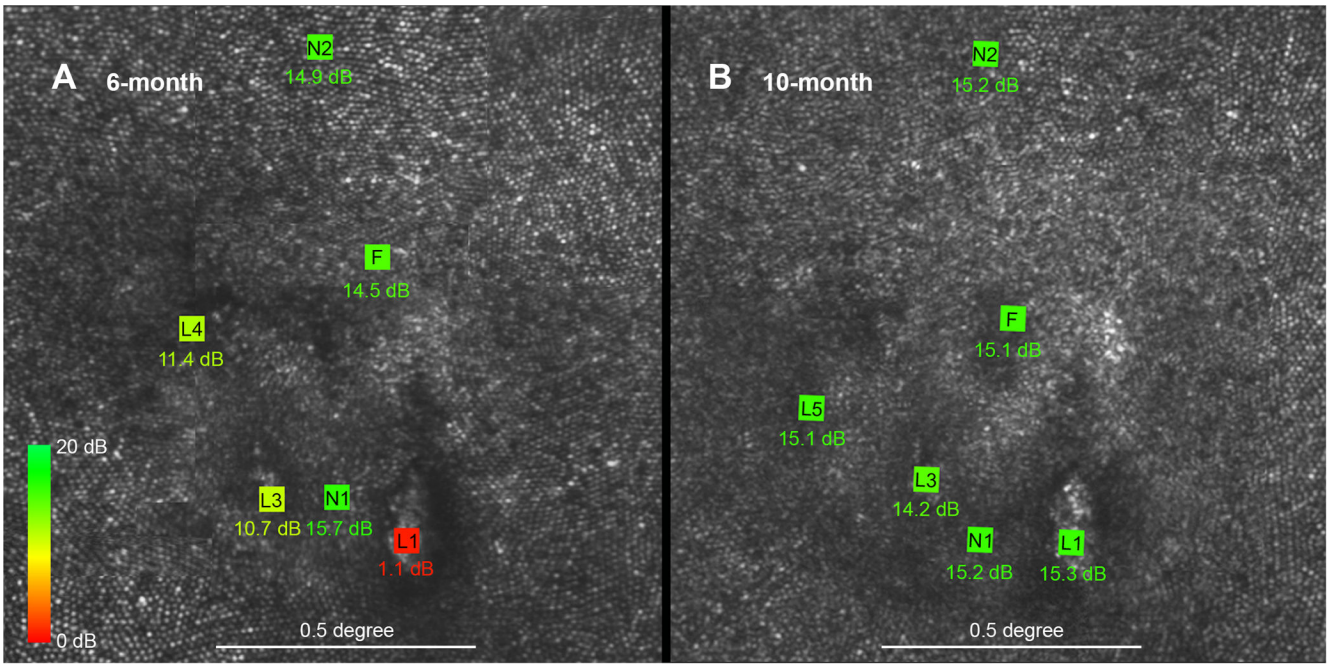

Figure 5.

Adaptive optics scanning laser ophthalmoscope confocal images from research visit 3 and 4 with adaptive optics microperimetry results. The size, color and location of the squares indicated the 3 arcminutes stimulus size, the delivery locations on the retina, and relative retinal sensitivity, respectively. Values of detection sensitivity in decibels (dB) were shown next to each test location. Fovea location (F) was determined with preferred retinal locus measurement. Normal 1 (N1) and fovea locations were slightly different between the 2 visits. Lesion 1 (L1), lesion 3 (L3), normal 2 (N2) were at the same location.